

PROPERTIES OF COHERENT MATTER-WAVE BUBBLES*

O. Zobay¹, B. M. Garraway²*Sussex Centre for Optical and Atomic Physics, University of Sussex,
Brighton BN1 9QH, United Kingdom*

Received 28 April 2000, accepted 4 May 2000

Recently we have proposed a method to create thin matter-wave bubbles from coherent atoms trapped in a magnetic potential. In this article we discuss in detail some properties of these states. In particular, we numerically and analytically investigate the Wigner function to demonstrate their non-classical nature. Furthermore, we study the energy and lifetime of the bubbles, which are long-lived resonances in a radio frequency-induced adiabatic potential, and illustrate how they can be transformed into excited eigenstates of the original harmonic trapping potential.

PACS: 42.50.Vk, 03.75.Be, 32.80.Pj, 03.75.Fi

1 Introduction

In a recent paper [1] we have proposed a mechanism for the generation of matter-wave bubbles from trapped coherent atoms. These bubbles could have applications as probes of condensate interactions, as an exotic environment for atoms, and as a candidate for a 2D condensate. In this paper we wish to explore some of the properties of these matter wave states to reveal part of their non-classical nature.

The bubbles can be formed using a variation of the well-established evaporative cooling technique (see Fig. 1). In evaporative cooling, magnetically trapped atoms are exposed to a strong radio frequency (RF) field that couples the bound hyperfine sublevel to an untrapped state. The motion of the atoms can then be pictured to take place in the adiabatic potential V_- of Fig. 1. With the RF frequency chosen appropriately, only the hottest atoms can reach and cross the maximum of the potential V_- , i.e., the resonance region of the RF-induced coupling, and get expelled from the trap. This mechanism leads to the cooling of the sample.

A completely different dynamical behaviour is to be expected if the atoms are evolving in the upper adiabatic potential V_+ . In particular, if they can be prepared in the quantum mechanical ground state of this potential, the resulting wave function has the shape of a shell or a bubble. In an anisotropic harmonic trap the bubble will be centered around the surface of an ellipsoid, in

*Presented at 7th Central-European Workshop on Quantum Optics, Balatonfüred, Hungary, April 28 – May 1, 2000.

¹E-mail address: o.zobay@sussex.ac.uk

²E-mail address: b.m.garraway@sussex.ac.uk

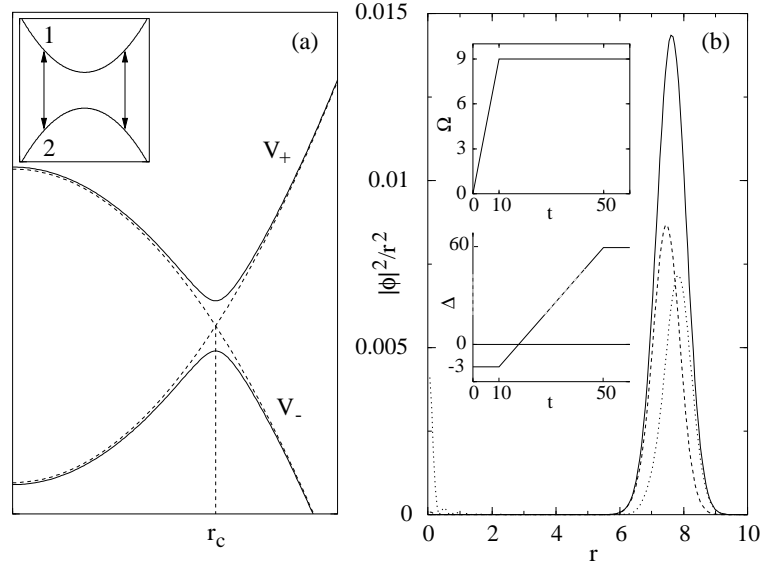


Fig. 1. (a) Schematic of field-induced adiabatic potentials V_{\pm} for $\Delta > 0$. Dashed curves show the bare potentials crossing at r_c . Inset: bare potentials showing resonance at r_c . (b) Matter-wave bubble prepared in the adiabatic potential V_+ of (a). Full curve: atomic density $|\phi_+|^2/r^2$ in the adiabatic state +; dotted and dashed curves show $|\phi_1|^2/r^2$ and $|\phi_2|^2/r^2$, respectively. The inset indicates the preparation process.

the isotropic case, which we will be considering in the following, the bubble is spherical. That it is indeed possible to create such matter-wave bubbles was shown in Ref. [1].

Before summarizing the creation process let us briefly outline the formal description of our system. We consider a sample of coherent atoms, e.g., a Bose-Einstein condensate, with two internal hyperfine ground states $|1\rangle$ and $|2\rangle$. These states are supposed to possess magnetic moments which are equal in magnitude but opposite in sign. In view of the spherical symmetry of our setup the two-component wave function of the system is written as $\Phi_i(\mathbf{r}) = \phi_i(r)/\sqrt{4\pi r}$. In an interaction picture with respect to the applied RF field the time evolution is determined by the Gross-Pitaevskii equation

$$\begin{aligned} i\dot{\phi}_1 &= \left(-\frac{1}{2} \frac{\partial^2}{\partial r^2} + \frac{r^2}{2} - \frac{\Delta(t)}{2} \right) \phi_1 + \Omega(t) \phi_2 + (g_{11}|\phi_1|^2 + g_{12}|\phi_2|^2) \frac{\phi_1}{r^2}, \\ i\dot{\phi}_2 &= \left(-\frac{1}{2} \frac{\partial^2}{\partial r^2} - \frac{r^2}{2} + \frac{\Delta(t)}{2} \right) \phi_2 + \Omega(t) \phi_1 + (g_{12}|\phi_1|^2 + g_{22}|\phi_2|^2) \frac{\phi_2}{r^2}. \end{aligned} \quad (1)$$

In these equations all quantities are scaled to natural units, i.e., harmonic oscillator frequency ω and oscillator length a_{ho} . The wave function is normalized according to $\int_0^\infty dr (|\phi_1|^2 + |\phi_2|^2) = N$, with N the total number of atoms. The coupling strength of the applied RF field is denoted $\Omega(t)$. Its effective detuning is defined by $\Delta(t) = (\hbar\omega_f - \Delta E(0))/\hbar\omega$, where $\Delta E(0)$ is the energy difference between the two hyperfine states at the origin $r = 0$ and ω_f the RF frequency. The nonlinearity parameters for the Gross-Pitaevskii equation are given by $g_{ij} = a_{ij}/a_{ho}$ with

a_{ij} the scattering lengths for intra- and inter-species collisions. In this paper, however, we will not give further consideration to the nonlinear effects. Note that in Eqs. (1) we have not taken the influence of gravity into account which might lead to a displacement between the extrema of the magnetic potentials for the two states $|1\rangle$ and $|2\rangle$ (“gravitational sag”). This effect may be compensated for by applying an additional optical dipole potential whose center (including the gravitational shift) coincides with the minimum of the magnetic field.

The creation of matter-wave bubbles now proceeds as shown in the inset of Fig. 1(b). Starting from a BEC prepared in the internal state $|1\rangle$ and in the ground state of the uncoupled trap the RF field is ramped up at negative detuning $\Delta(t)$ to a sufficiently large value of $\Omega(t)$. This allows for a smooth transition of the wave function from the bare trapping field into the adiabatic potential

$$V_+(r, t) = \sqrt{[r^2 - \Delta(t)]^2/4 + \Omega^2(t)}, \quad (2)$$

defined as the spatially dependent (high-energy) eigenvalue of the potentials and couplings in Eqs. (1). Subsequently, the detuning is increased to the desired final value at fixed Ω . If the process is performed slowly enough, the wave function will always stay in the instantaneous ground state of V_+ due to adiabatic following. This ground state has a finite lifetime which, however, increases exponentially for growing Ω (see Sec. 3). In this way, a long-lived bubble state, e.g., as shown in Fig. 1(b), can be produced.

In this paper we discuss some of the properties of these states, in particular, we investigate their non-classicality by studying their Wigner function.

2 Wigner function

The Wigner function provides a very useful tool for the study of quantum states. The general features reflect a phase space distribution for a quantum state, i.e., a quasi-probability distribution. However, the negativity of the function provides an indication of non-classical behaviour, while integration over an infinite line gives the correct marginal distributions. Thus to investigate the non-classical nature of our bubble state, we will calculate the Wigner function.

For a three-dimensional wave function the Wigner function takes the form [2]

$$W(\mathbf{r}, \mathbf{p}) = \frac{1}{(2\pi)^3} \int d\mathbf{q} \Psi^*(\mathbf{r} + \mathbf{q}/2) \Psi(\mathbf{r} - \mathbf{q}/2) e^{i\mathbf{p}\cdot\mathbf{q}}. \quad (3)$$

Our matter wave bubble is spherically symmetric, i.e. $\Psi(\mathbf{r}) \rightarrow \Psi(r)$, which means that if we let \mathbf{r} define the z -axis, with θ as the angle between \mathbf{r} and \mathbf{p} and θ' as the angle between \mathbf{r} and \mathbf{q} , the equation (3) reduces to

$$\begin{aligned} W(\mathbf{r}, \mathbf{p}) = W(r, p, \theta) &= \frac{1}{(2\pi)^2} \int_0^\infty dq \int_{-1}^1 dx q^2 \\ &\times \Psi^*(\sqrt{r^2 + q^2/4 + rqx}) \Psi(\sqrt{r^2 + q^2/4 - rqx}) \\ &\times \exp(ixqp \cos \theta) J_0(qp \sin \theta \sqrt{1 - x^2}) \end{aligned} \quad (4)$$

when we carry out the integration over the polar angle ϕ' relative to \mathbf{r} and \mathbf{q} . In Eq. (4) J_0 denotes the Bessel function of order 0 and $x = \cos \theta'$.

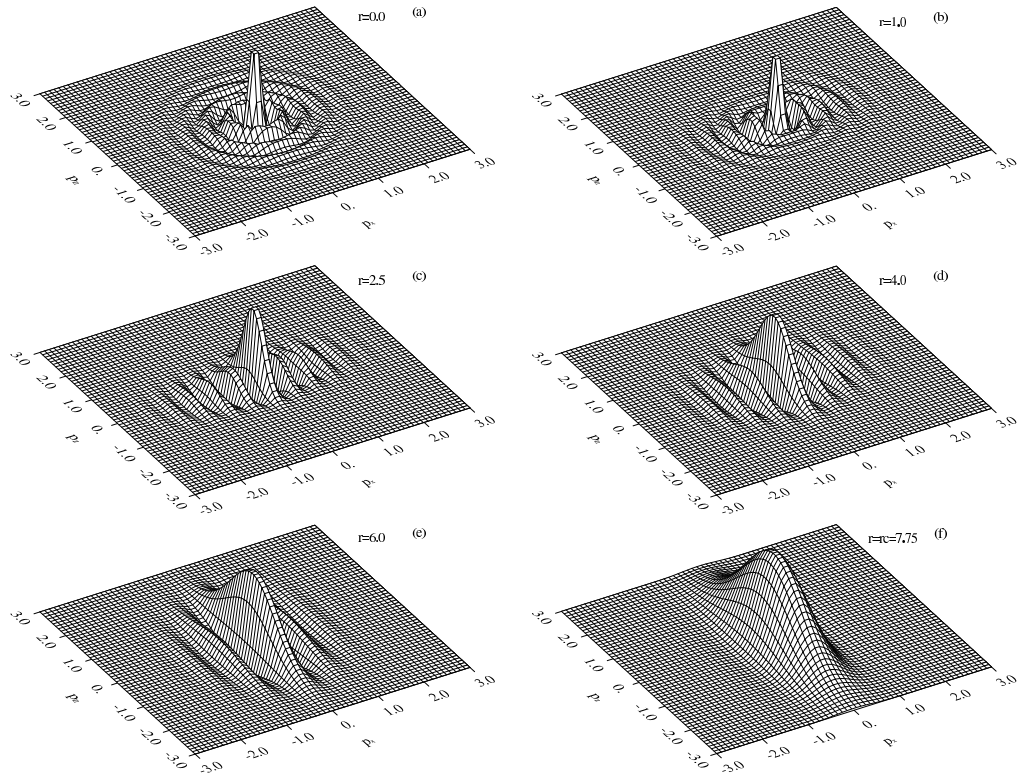


Fig. 2. Wigner function as a function of p and θ at fixed $r = 0.0, 1.0, 2.5, 4.0, 6.0,$ and 7.75 for the bubble state with $\Omega = 9$ and $\Delta = 60$.

To accurately determine the Wigner function for the bubble state, Eq. (4) was evaluated numerically with a wave function $\Psi(r) = \Phi_+(r)$ previously obtained from the integration of Eqs. (1). In the examples shown in Figs. 2 and 3 the state depicted in Fig. 1(b) was used, which has parameters $\Omega = 9$ and $\Delta = 60$ for the potential. Because the Wigner function for a spherically symmetric wave function depends on three variables it is hard to display the numerical results. As a result we have chosen to make two types of section through the distribution. Figures 2 show the Wigner function for fixed r as a function of the projections of \mathbf{p} on \mathbf{r} , i.e., as functions of p_z and p_x . In Figs. 3, on the other hand, the roles of p and r are interchanged, i.e., we see the Wigner function at fixed p as a function of r_z and r_x which are the projections of \mathbf{r} onto \mathbf{p} .

To obtain a deeper understanding of the structures shown in these figures we have investigated an analytically tractable “model bubble” system. To this end, we approximate the wave function as a radial Gaussian function

$$\phi_+(r) \approx \frac{1}{\sqrt[4]{\pi\sigma^2}} \exp\left[-\frac{(r-r_c)^2}{2\sigma^2}\right]. \quad (5)$$

In Eq. (5) it is understood that $\phi_+(r=0) = 0$. For given Ω and Δ the bubble radius is determined

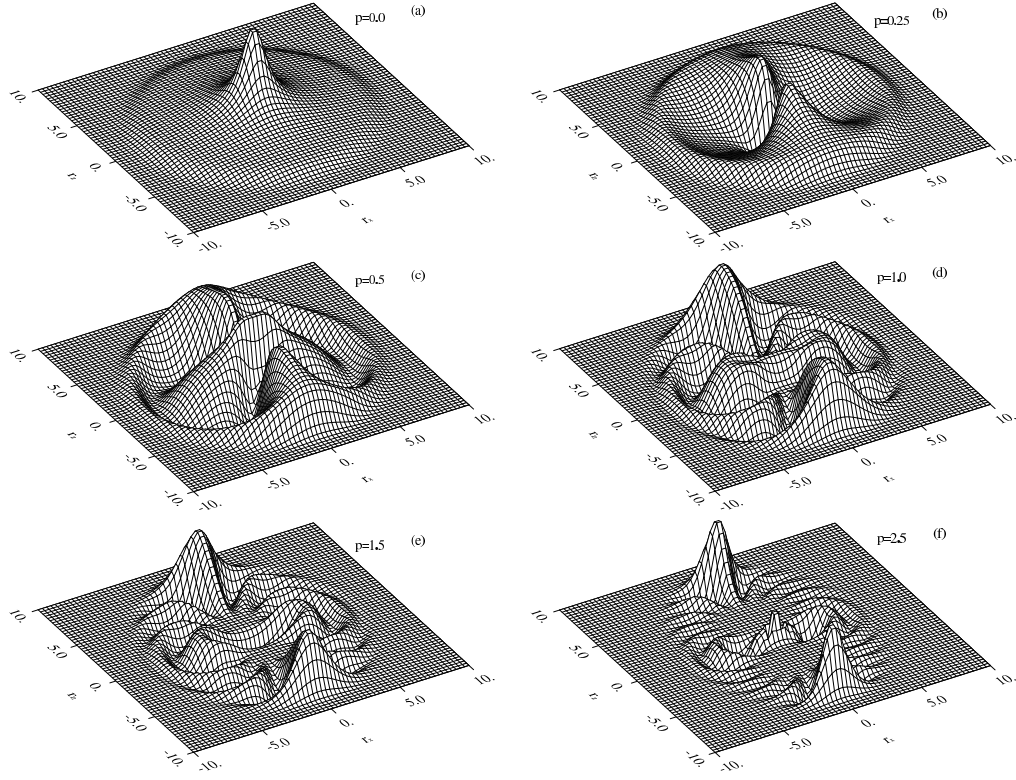


Fig. 3. Wigner function as a function of q and θ at fixed $p = 0.0, 0.25, 0.5, 1.0, 1.5,$ and 2.5 for the bubble state with $\Omega = 9$ and $\Delta = 60$.

by $r_c = \sqrt{\Delta}$. Expanding the adiabatic potential around r_c , i.e., $V_+(r) \approx \Omega + \Delta(r - r_c)^2/2\Omega$, we can identify $\sigma = (\Omega/\Delta)^{1/4}$. The approximate description should be valid if the bubble radius is large compared to its thickness, i.e., $r_c \gg \sigma$ or $\Delta^3 \gg \Omega$. This condition is assumed to hold in the following. In the numerical example, we have $r_c = 7.75$ and $\sigma = 0.62$. Under these circumstances we find the following behaviour of the Wigner function.

1. At $r = 0$ the angle θ is not defined. We obtain

$$W(r = 0, p) = \pi^{-3} \exp(-\sigma^2 p^2/4) j_0(2r_c p) \quad (6)$$

with the spherical Bessel function $j_0(x) = \sin x/x$. The Wigner function is thus oscillating with a period determined by r_c . These oscillations, which indicate the non-classical nature of the state, decay on a scale given by $1/\sigma$ [compare with Fig. 2(a)].

2. To determine the Wigner function inside the bubble, i.e., $r \lesssim r_c - \sigma$, we expand

$$\begin{aligned} & \Psi^*(\sqrt{r^2 + q^2/4 + rqx}) \Psi(\sqrt{r^2 + q^2/4 - rqx}) \\ & \simeq \exp\{-\eta [(q - 2q_0)^2/4 + r^2 x^2]\} / 4\pi r_c^2 \sqrt{\pi\sigma^2} \end{aligned} \quad (7)$$

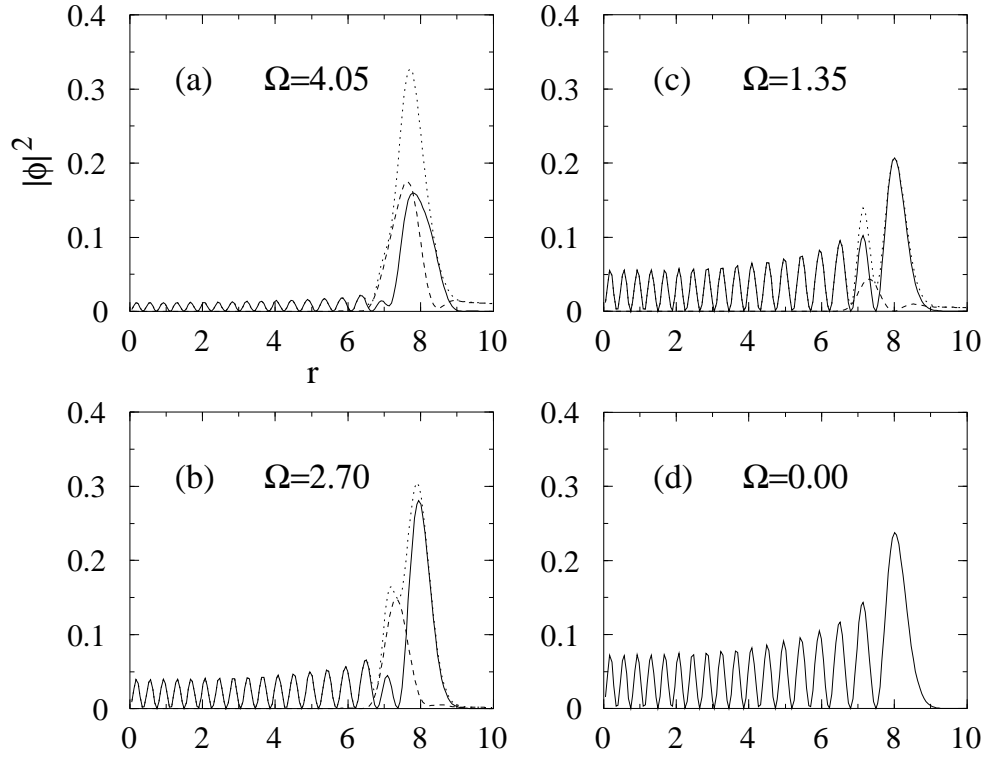


Fig. 4. Resonance states of Eqs. (1) at $\Delta = 60$ and various values of Ω . The wave functions are determined numerically by slowly decreasing the value of Ω in Eqs. (1) after initially preparing a bubble state. Full curves: $|\phi_1|^2$, dashed: $|\phi_2|^2$, dotted: sum of both. The displayed wave functions are normalized to one.

with $\eta = (r_c^2 - r^2)/r_c^2\sigma^2$ and $q_0 = \sqrt{r_c^2 - r^2}$. For small $p \sin \theta$ one can make the substitution $J_0(p \sin \theta \sqrt{1 - x^2}) \simeq J_0(2p \sin \theta q_0)$. For the Wigner function it is thus obtained

$$W(r, p, \theta) = \frac{q_0}{2\pi^3 r_c} \sqrt{\frac{\pi}{\alpha}} \exp(-\beta^2/4\alpha) J_0(2q_0 p \sin \theta) \text{Re erf}(\sqrt{\alpha} + i\beta/2\sqrt{\alpha}) \quad (8)$$

with $\text{erf} x$ the error function, $\alpha = \eta q^2 + (p \cos \theta)^2/\eta$, and $\beta = 2q_0 p \cos \theta$. In particular, for $\theta = 0$, the Bessel function does not play a role, and we see that at fixed r , $W(r, p, \theta = 0)$ is essentially a Gaussian in p . For smaller r this Gaussian is modulated by slight oscillations induced by the error function, but these oscillations die away as r grows and the error function becomes constant. This behaviour is clearly demonstrated in Figs. 2. Finally, we also note that $W(r, p = 0) > |W(r, p, \theta)|$, and, from Eq. (8), $W(r, p = 0)$ is a monotonically decaying function of r [see Fig. 3(a)].

3. For larger $p \sin \theta$ we replace the Bessel function in Eq. (4) by its asymptotic expansion thereby still neglecting its dependence on x . Together with Eq. (7) this yields the result

$$W(r, p, \theta) = \frac{(r_c^2 - q^2)^{1/4}}{16\pi^3 r_c \sqrt{\alpha p \sin \theta}} \operatorname{Re} \left\{ \exp \left[-\frac{(p \sin \theta)^2}{\eta} - \frac{\gamma^2}{4\alpha} + 2iq_0 p \sin \theta - i\frac{\pi}{4} \right] \times [\operatorname{erf}(\sqrt{\alpha} + i\gamma/2\sqrt{\alpha}) - \operatorname{erf}(-\sqrt{\alpha} + i\gamma/2\sqrt{\alpha})] \right\} \quad (9)$$

with $\gamma = 2q_0 p \cos \theta + ip^2 \sin(2\theta)/\eta$. Typically, the approximations (8) and (9) have an overlapping region of good accuracy, e.g., at intermediate p for fixed q and θ . At $\theta = \pi/2$ Eq. (9) simplifies to

$$W(r, p, \theta = \pi/2) = \frac{(r_c^2 - q^2)^{1/4}}{8\pi^3 r_c \sqrt{\alpha p}} \exp(-p^2/\eta) \cos(2q_0 p - \pi/4) \operatorname{erf} \sqrt{\alpha}. \quad (10)$$

We see that at fixed r , W considered as a function of p has still a Gaussian-shaped envelope, but in contrast to the case $\theta = 0$ this envelope is strongly modulated by oscillations induced by the cosine appearing in Eq. (10). Only if r gets close to r_c the period of these oscillations grows rapidly and they become less and less manifest in the shape of the Wigner function. Again, these conclusions are corroborated in Figs. 2. In Fig. 2(f) we see that when $r = r_c = 7.75$ we have an almost Gaussian distribution in p_z and p_x . The Wigner function is broader in the z -direction because at $q = r_c$ the matter wave is more confined in the radial direction than it is in the transverse direction.

4. For $r > r_c$ the exponent appearing in Eq. (4) after insertion of the wave function (5) has to be expanded around $q = x = 0$. For this case we only give the result

$$W(r, p = 0) = \frac{\sigma^2}{4\pi^3 r (r - r_c)} \exp[-(r - r_c)^2/\sigma^2] \quad (11)$$

which shows (as $W(r, p = 0) > |W(r, p, \theta)|$) that the Wigner function is exponentially decaying outside the bubble.

The plots of the Wigner function at fixed p , i.e., Figs. 3, complement our above discussion of W which focussed on the behaviour with p at fixed q . For $p = 0$ the Wigner function is everywhere positive and monotonically decaying with q as discussed under 2 above. For small momentum $p > 0$ some structure develops in the center thereby evidently displaying negativity for small q . As p is increased the structure becomes more complex and exhibits curved fringes when p reaches 1.0 [Fig. 3(d)]. Further increases in p result in smaller, but even more complex curved structures, until at $p = 2.5$ [Fig. 3(f)] we find essentially two lobes of probability distribution, located at $(r_x \sim 0, r_z \sim \pm r_c)$, with a fringed structure isolated in the centre. This distribution is rather reminiscent of the Wigner function of the even and odd coherent states [3], but the suggestion here is that the lobes arise from opposite parts of the bubble, and the fringes are the result of quantum interference between them.

It should be noted that the analytical expressions given above for the Wigner function also allow to estimate the influence of the nonlinear interactions included in Eqs. (1). As these interactions tend to broaden the wave function due to the interatomic repulsion, their effect can be studied in a simple way by investigating the behaviour of W as the width parameter σ is increased.

3 Energy and lifetime

The bubble states are not truly bound states with an infinite lifetime. Rather, they should be considered resonances, albeit long-lived ones, of the adiabatic potential V_+ . This feature becomes obvious if Eqs. (1) are transformed to the dressed state basis, i.e., the basis that diagonalizes the bare potentials and the couplings at each point r [4]. This representation shows that the two adiabatic wave function components ϕ_+ and ϕ_- are coupled by kinetic terms. These terms, however, become less important for growing Ω . The decay rate γ of the bubble may be determined with the help of semiclassical methods developed in connection with molecular predissociation [4, 5]. Applying these techniques we find that $\gamma = -2\text{Im} E_0$, where the complex ground state energy E_0 is a solution of

$$[e^{2\pi\delta(E)} - 1] \cos \Phi(E) e^{-i[\beta(E) - \Phi(E)]} + \cos \beta(E) = 0 \quad (12)$$

with $\beta(E) = \pi(2E + \Delta - 1)/4$ and the quantities $\delta(E)$ and $\Phi(E)$ characterizing the scattering matrix of the linearized potential crossing problem. For these quantities there are several analytical approximations in the literature [6]; following, e.g., Ref. [4] one can put $\delta(E) = 1/8ab$ and $\Phi(E) = 2b^3/3a + \arg\Gamma[i\delta(E)] + \delta(E) \ln[\delta(E)] - 2\delta(E) \ln(b/a) + \pi/4$ with $a^2 = \Delta/(8\Omega^3)$ and $b^2 = E/\Omega$. For large enough Ω , i.e., $\exp[2\pi\delta(E)] \gg 1$, one obtains

$$\gamma = \frac{2 \cos^2 \beta(E)}{\{\exp[2\pi\delta(E)] - 1\}(\partial\Phi/\partial E)} \quad (13)$$

where all quantities have to be evaluated at the approximate energy of the bubble

$$\text{Re } E_0 \simeq \Omega + \sqrt{\Delta/4\Omega}. \quad (14)$$

This estimate for the energy follows directly from the harmonic expansion of V_+ around its minimum at r_c . Equation (14) can be expected to be accurate over a large range of Ω as the bubble width only grows with $\Omega^{1/4}$. Equation (13) leads to two important conclusions. First of all, the decay is exponentially suppressed with growing Ω . Secondly, for $\text{Re } E_0 = 2k + 3/2 - \Delta/2$ with integer k the decay rates become very small. In these cases the matter-wave bubble is in resonance with an eigenstate of the bare harmonic trapping potential. This stabilization effect may be used to obtain extremely long-lived states already for moderate coupling strengths.

So far we have considered the case of strong coupling, i.e., Ω large enough that the concept of adiabatic potentials is meaningful and the bubble is well localized at the bottom of V_+ . However, it is also of interest to study the system behaviour when, at fixed detuning Δ , the coupling strength Ω is lowered to zero. It turns out that resonance states exist at all values of Ω – although some have relatively short lifetime – but their qualitative character is changed profoundly as it is displayed in Figs. 4. For smaller values of Ω the wave function evolves into an eigenstate of the bare harmonic potential. In Ref. [1] it was proposed to use this method to experimentally prepare atoms in high-lying trap eigenstate. From Figs. 4 we can distinguish, at $\Delta = 60$, two different phases in this process. In the first stage, represented by Fig. 4(a) [compare to Fig. 1(b)], the original maximum in the wave function which constitutes the bubble more or less maintains its shape. The two components ϕ_1 and ϕ_2 continue to have approximately equal weight and the adiabatic description is still applicable. At the same time, a smaller part of the wave function begins to fill the interior of the shell thereby already displaying oscillatory structures characteristic

of the bare trap eigenstate. In the second phase, shown in Figs. 4(b)-(c) the bubble itself begins to disintegrate, the component ϕ_2 starts to vanish whereas the inner oscillatory structures continue to grow. The resonance is most unstable, i.e., the lifetime γ^{-1} is lowest, around $\Omega \approx 4$ which here coincides with the beginning of the disintegration process and the change in character of the resonance.

The lifetime of the resonances in the limit of low coupling, i.e., $\exp[2\pi\delta(E)] - 1 \ll 1$, is given by

$$\gamma = 4\{\exp[2\pi\delta(E)] - 1\} \cos^2 \Phi(E)/\pi. \quad (15)$$

Again, all quantities have to be evaluated at the energy of the resonance, which in this case can be taken as the energy of the emerging eigenstate in the bare trap to a good degree of approximation. It is an interesting question as to which harmonic eigenstate the resonance actually evolves into. Of course, it can immediately be answered by numerically solving Eq. (12). We have not been able to give a simple qualitative argument, though. As a rule of thumb, we find that around $\Delta = 20$ the resonance evolves into the second eigenstate with positive energy, i.e., $(2n-1/2) - \Delta/2 \approx 2.5 \dots 4.5$ with n the number of radial nodes of $\phi_1(r)$. Around $\Delta = 60$ we find $(2n-1/2) - \Delta/2 \approx 4.5 \dots 6.5$, i.e., evolution into the third eigenstate of positive energy [compare with Fig. 4(d), where $n = 18$].

4 Conclusion

In this paper we have extended our initial study [1] on the creation and properties of coherent matter-wave bubbles. Here we have put the emphasis on elucidating the non-classical nature of these states by analytically and numerically investigating their Wigner function. The Wigner function displays pronounced negativity which implies that the bubbles cannot be considered as “quasi-classical objects”. In this context we wish to mention that we are not aware of other detailed discussions of the Wigner function of genuine three-dimensional quantum states.

Furthermore we have studied the energy and lifetime of the matter-wave bubbles which are resonance states in the RF-included adiabatic potential. We have illustrated the transformation from bubble state to harmonic trap eigenfunction that occurs when the field intensity is reduced to zero.

Acknowledgments This work was supported by the United Kingdom Engineering and Physical Sciences Research Council.

References

- [1] O. Zobay and B.M. Garraway: submitted
- [2] E.P. Wigner: *Phys. Rev.* **40** (1932) 749; see also M. Hillery, R.F. O’Connell, M.O. Scully, E.P. Wigner: *Phys. Rep.* **106** (1984) 121
- [3] V. Buzek and P.L. Knight: *Opt. Commun.* **81** (1991) 331; *Progress in Optics* **34**, ed. E. Wolf, North Holland, Amsterdam, 1995, p.1
- [4] A. D. Bandrauk and M. S. Child: *Molec. Phys.* **19** (1970) 95
- [5] M. S. Child: *Molecular Collision Theory*, Academic, London, 1974
- [6] C. Zhu and H. Nakamura: *J. Chem. Phys.* **98** (1993) 6208